ISSN 1070-3284, Russian Journal of Coordination Chemistry, 2016, Vol. 42, No. 4, pp. 267–273. © Pleiades Publishing, Ltd., 2016.
Original Russian Text ©A.S. Burlov, V.G. Vlasenko, Yu.V. Koshchienko, S.I. Levchenkov, I.V. Pankov, Ya.V. Zubavichus, A.L. Trigub, G.S. Borodkin, T.A. Mazepina, D.A. Garnovskii, A.I. Uraev, 2016, published in Koordinatsionnaya Khimiya, 2016, Vol. 42, No. 4, pp. 237–244.

Binuclear Metallochelates of 2-(N-Tosylamino)benzal-2'-(Hydroxymethyl)aniline: Syntheses, Structures, and Magnetic Properties

A. S. Burlov[a], *, V. G. Vlasenko[b], Yu. V. Koshchienko[a], S. I. Levchenkov[c], I. V. Pankov[a], Ya. V. Zubavichus[d], A. L. Trigub[d], G. S. Borodkin[a], T. A. Mazepina[a], D. A. Garnovskii[c], and A. I. Uraev[a]

[a] *Research Institute of Physical and Organic Chemistry, Southern Federal University, Rostov-on-Don, Russia*

[b] *Research Institute of Physics, Southern Federal University, Rostov-on-Don, Russia*

[c] *Southern Scientific Center, Russian Academy of Sciences, Rostov-on-Don, Russia*

[d] *Kurchatov Institute Russian Research Center, pl. Kurchatova 1, Moscow, 123182 Russia*

**e-mail: anatoly.burlov@yandex.ru*

Received July 22, 2015

Abstract—Binuclear complexes of Co(II), Cu(II), and Pd(II) with 2-(N-tosylamino)benzal-2'-(hydroxymethyl)aniline are synthesized. The compositions and structures of the ligand and complexes are determined from the data of elemental analysis, IR spectroscopy, ^{1}H, ^{13}C, and ^{15}N NMR spectroscopy, X-ray absorption spectroscopy, and magnetochemical measurements in a temperature range of 294–77.4 K. All complexes are dimeric. The Cu···Cu and Co···Co distances equal to 3.03 and 2.99 Å, respectively, are obtained for the Cu(II) and Co(II) complexes. These complexes are characterized by the antiferromagnetic exchange interaction with $2J = -630$ and -42 cm^{-1}, respectively.

DOI: 10.1134/S1070328416030027

INTRODUCTION

The tridentate Schiff bases containing protonated groups (XH and YH) in the *ortho* positions of the phenyl rings are among the main objects of coordination chemistry and provide wide possibilities for the variation of the compositions and structures of the complexes obtained from these Schiff bases.

The complexes based on the tridentate Schiff bases are recently being considered as potential magnetically active [1–8], catalytic [9, 10], and optical materials [11, 12].

Metallochelates of tridentate and polydentate azomethine ligands of 2-hydroxy- and 2-tosylaminobenzaldehyde derivatives, their substituted derivates, 4-formyl-3-methyl-1-phenylpyrazol-5-one (or thione), and *ortho*-aminophenols and *ortho*-aminothiophenols [13–23]; monosubstituted *ortho*-phenylenediamines [24–30]; sterically hindered 4,6-di-*tert*-butyl-2-aminophenols [31–33]; and 2-amino-3-hydroxypyridine [34], 2-tosylaminoaniline [20], amino alcohols [13, 35], 1,3-diaminopropanol [36], and 1-aminobenzimidazole and its 2-substituted derivatives [26] are of special interest.

Bi- and polynuclear structures with antiferromagnetic or ferromagnetic exchange interactions between metal atoms are observed in these metal complexes, depending on the ligand nature.

Several reviews are devoted to the syntheses and specific features of magnetic exchange in the bi- and polynuclear metal complexes with azomethines and hydrazones [13, 14, 37, 38].

The results of the syntheses and studies of the structures and magnetic properties of the Cu(II) (**Ia**), Co(II) (**Ib**), and Pd(II) (**Ic**) binuclear complexes with the tridentate azomethine ligand, 2-(N-tosylamino)benzal-2'-(hydroxymethyl)aniline (H_2L), are presented in this work.

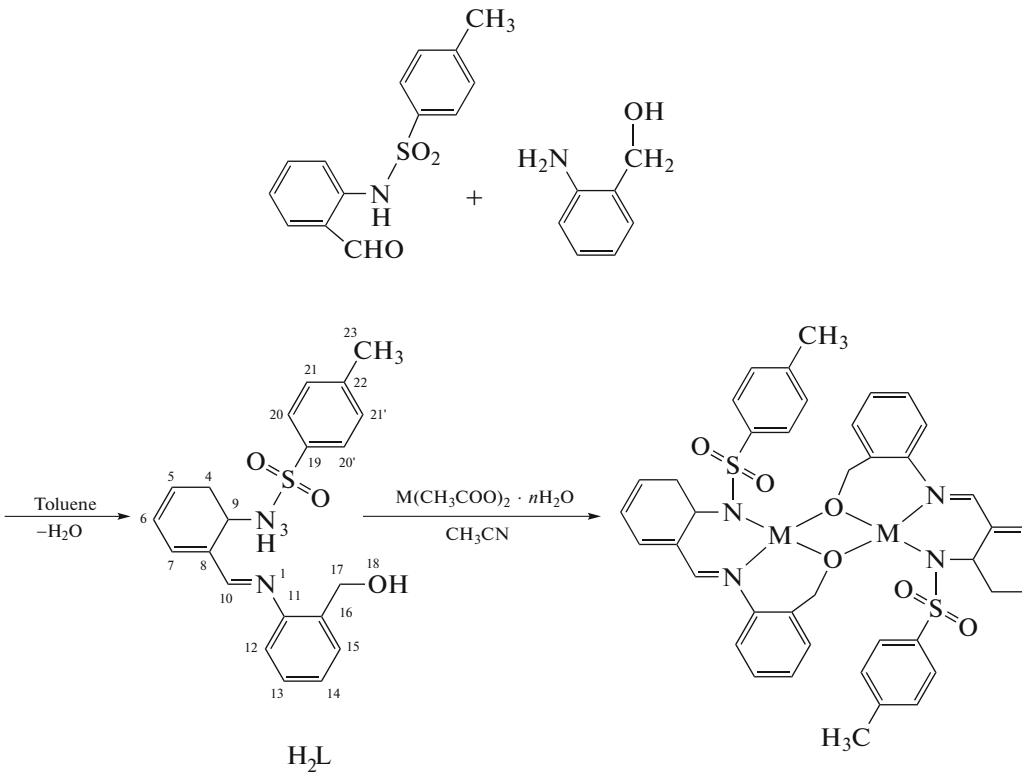

H_2L

I: M = Cu (a), Co (b), Pd (c)

EXPERIMENTAL

2-(Hydroxymethyl)aniline (Alfa Aesar) was used without additional purification in the synthesis of azomethine ligand H_2L. 2-(N-Tosylamino)benzaldehyde was prepared according to a described procedure [39]. Commercially available copper acetate monohydrate, cobalt acetate tetrahydrate, and palladium acetate were used in the syntheses of complexes **I**.

Synthesis of H_2L. 2-Hydroxymethylaniline (0.24 g, 2 mmol) in toluene (10 mL) was added to a solution of 2-(N-tosylamino)benzaldehyde (0.55 g, 2 mmol) in toluene (20 mL). The mixture was refluxed with the Dean–Stark trap until the complete separation of water within 2 h. The solvent was distilled off to 1/3 of the volume, and ethanol (10 mL) was added. The precipitated azomethine was filtered off and recrystallized from an ethanol–toluene (2 : 1) mixture. The yield of pale-yellow fine crystals was 97%, mp = 132–133°C.

For $C_{21}H_{20}N_2O_3S$

anal. calcd., %:	C, 66.30;	H, 5.30;	N, 7.36.
Found, %:	C, 66.51;	H, 5.35;	N, 7.28.

^{1}H NMR (300 MHz, $CDCl_3$), δ, ppm: 2.34 (3H, s, CH_3), 2.74 (1H, t, J = 5.0 Hz, OH), 4.95 (2H, d, J = 5.1 Hz, CH_2), 7.06 (1H, t, J = 5.0 Hz, H^6), 7.17–7.23 (3H, m, H^{12}, H^{21}, $H^{21'}$), 7.31–7.44 (4H, m, H^5, H^7, H^{13}, H^{14}), 7.52 (1H, d, J = 7.2 Hz, H^{15}), 7.61 (1H, d, J = 8.4 Hz, H^4), 7.82 (2H, d, J = 8.4 Hz, H^{20}, $H^{20'}$), 8.60 (1H, s, CH^{10}=N), 13.19 (1H, s, NH). ^{13}C NMR (150 MHz, $CDCl_3$), δ, ppm: 21.48 (C^{23}), 62.16 (C^{17}), 116.97 (C^{12}), 117.19 (C^4), 120.83 (C^8), 122.42 (C^6), 127.30 (C^{20}), 127.58 (C^{14}), 129.01 (C^{13}), 129.64 (C^{15}), 129.69 (C^{21}), 132.36 (C^5), 134.27 (C^7), 135.34 (C^{16}), 136.92 (C^{19}), 139.56 (C^9), 143.80 (C^{22}), 146.82 (C^{11}), 161.35 (C^{10}). ^{13}N NMR (150 MHz, $CDCl_3$), δ, ppm: 122.32 (N^3), 306.60 (N^1).

IR (ν, cm^{-1}): 3424 sh (NH), 2921 sh (OH), 3035–2870 (CH_2), 1616 (CH=N), 1341 $\nu_{as}(SO_2)$, 1156 $\nu_s(SO_2)$.

Synthesis of complexes Ia–Ic. Copper acetate monohydrate (0.2 g, 1 mmol) or cobalt acetate tetrahydrate (0.25 g, 1 mmol) in acetonitrile (10 mL), or palladium acetate (0.22 g) in acetone (10 mL) was added to a solution of H_2L (0.38 g, 1 mmol) in acetonitrile (20 mL). The mixture was refluxed for 2 h. The precipitated complexes were filtered off, washed two times with acetonitrile (each portion of 5 mL), and dried in a vacuum drying box at 150°C.

Bis{[2-(N-tosylamino)benzal-2'-(hydroxymethyl)anilinato]copper} (**Ia**): dark brown powder, 69% yield, mp > 250°C (decomp.).

For $C_{42}H_{36}N_4O_6S_2Cu_2$

anal. calcd., %:	C, 57.07;	H, 4.10;	N, 6.34;	Cu, 14.38.
Found, %:	C, 57.18;	H, 4.21;	N, 6.42;	Cu, 14.29.

IR (powder, ν, cm^{-1}): 3018–2850 w (CH_2), 1609 s (CH=N), 1296 s $\nu_{as}(SO_2)$, 1137 vs $\nu_s(SO_2)$; μ_{eff} = 0.88 μ_B (294 K)–0.51 μ_B (77.4 K).

Bis{[2-(N-tosylamino)benzal-2'-(hydroxymethyl)anilinato]cobalt} (**Ib**): brown powder, 75% yield, mp > 250°C (decomp.).

For $C_{42}H_{36}N_4O_6S_2Co_2$

anal. calcd., %:	C, 57.67;	H, 4.15;	N, 6.40;	Co, 13.47.
Found, %:	C, 57.39;	H, 4.56;	N, 6.52;	Co, 13.72.

IR (ν, cm^{-1}): 3068–2824 w (CH_2), 1612 s (CH=N), 1297 s $\nu_{as}(SO_2)$, 1138 vs $\nu_s(SO_2)$. μ_{eff} = 4.42 μ_B (294 K)–3.54 μ_B (77.4 K).

Bis{[2-(N-tosylamino)benzal-2'-(hydroxymethyl)anilinato]palladium} (**Ic**): yellow-brown powder, 72% yield, mp > 250°C (decomp.).

For $C_{42}H_{36}N_4O_6S_2Pd_2$

anal. calcd., %:	C, 52.02;	H, 3.74;	N, 5.78;	Pd, 21.95.
Found, %:	C, 52.12;	H, 3.85;	N, 5.63;	Pd, 22.26.

IR (ν, cm^{-1}): 3062–2844 (CH_2), 1610 m (CH=N), 1301 s $\nu_{as}(SO_2)$, 1144 $\nu_s(SO_2)$. ^{1}H NMR (300 MHz, $CDCl_3$), δ, ppm: 2.35 (6H, s, $2CH_3$), 4.20 (2H, s, J = 11.1 Hz, CH_2), 4.66 (2H, s, J = 11.1 Hz, CH_2), 5.78 (2H, d, J = 7.8 Hz, H^{12}), 6.98 (4H, d, J = 8.1 Hz, H^{21}, $H^{21'}$), 7.07 (2H, s, CH^{10}=N), 7.12–7.32 (12H, m, H^6, H^7, H^{10}, H^{13}, H^{14}, H^{15}), 7.51–7.56 (2H, m, H^5), 7.61 (4H, s, J = 8.4 Hz, H^{20}, $H^{20'}$), 7.75 (2H, d, J = 8.1 Hz, H^4). ^{13}C NMR (150 MHz, $CDCl_3$), δ, ppm: 21.31 (C^{23}), 68.37 (C^{17}), 120.81 (C^{12}), 124.51 (C^6), 126.70 (C^{20}), 128.45 (C^{13}), 128.79 (C^{14}), 128.90 (C^{21}), 130.46 (C^4), 130.48 (C^{15}), 134.32 (C^7), 134.90 (C^5), 140.77 (C^{22}), 140.89 (C^{19}), 143.60 (C^9), 144.29 (C^{11}), 161.95 (C^{10}). ^{15}N NMR (150 MHz, $CDCl_3$), δ, ppm: 76.7 (N^3), 206.30 (N^1).

Elemental analyses to C, H, and N were carried out on a Carlo Erba Instruments TCM 480 instrument. The metal content was analyzed using gravimetry. Attenuated total internal reflectance (ATR) powder IR spectra were recorded on a Varian Excalibur-3100 FT–IR instrument. ^{1}H NMR spectra were measured on a Varian Unity-300 spectrometer (300 MHz) for H_2L and **Ic**. ^{13}C and ^{15}N NMR spectra were recorded on a Bruker Avance-600 spectrometer (150 MHz) in a solution of $CDCl_3$. ^{1}H, ^{13}C, and ^{15}N chemical shifts are presented relative to residual signals of the deuterated solvent $CDCl_3$: 7.24 ppm for ^{1}H and 77.0 ppm for ^{13}C; 381.7 ppm for ^{15}N relative to the signal of CH_3NO_2.

X-ray absorption Cu and Co *K*-edge spectra for compounds **Ia** and **Ib** were obtained on the Structural Materials Science station at the Kurchatov Center of Synchrotron Radiation and Nanotechnologies (Moscow) [40]. The energy of the electron beam used as an X-ray synchrotron radiation source was 2.5 GeV at a current of 60–80 mA. A double crystal monochromator Si(111) was used for X-ray radiation monochromatization. The X-ray beam intensity before and after sample irradiation was measured using two ionization chambers filled with nitrogen–argon mixtures providing 20 and 80% of absorption for I_0 and I_t, respectively.

The obtained X-ray absorption spectra were processed using standard procedures of background isolation, normalization to the value of the *K*-edge jump, and isolation of atomic absorption μ_0 [41], after which the Fourier transform of the obtained EXAFS (χ) spectra was performed in the range of wave vectors of photoelectrons k from 2.6 to 12–13 $Å^{-1}$ with the weight function k^3. The obtained module Fourier transformants (MFT) of the χ spectra corresponded to the radial distribution function of the atoms around the absorbing metal atom with the accuracy to the phase shift. The threshold ionization energy (E_0) was chosen from the maximum of the first *K*-edge derivative and further was varied by fitting.

Exact values of the parameters of the nearest environment of metal atoms in the metal complexes were determined by nonlinear fitting of the parameters of the corresponding coordination spheres when comparing the calculated EXAFS signals and the signal isolated from the full EXAFS spectrum using the Fourier filtration method. The nonlinear fitting was carried out using the IFFEFIT program package [42]. Phases and amplitudes of photoelectron wave scattering necessary for model spectrum construction were calculated using the FEFF7 program [43]. The X-ray diffraction data for single crystals of the complexes with the close atomic environment of the metal atoms were used as the initial atomic coordinates necessary for the calculation of scattering phases and amplitudes and further fitting. The search for these structures was performed in the database of the Cambridge Crystallographic Data Centre.

In all cases, the number of parameters varied for multisphere fitting did not exceed the number of independent parameters N_{ind}, which can reliably be deter-

mined from a given EXAFS spectrum in specified ranges Δk and Δr provided by Eq. (1)

$$N_{\text{ind}} = (2\Delta r\Delta k/\pi) + 1, \quad (1)$$

where Δk is the analyzed region of the EXAFS spectrum in a space of wave vectors of a photoelectron, and Δr is the region of the R space in which the Fourier filtration is performed.

Function (2) was minimized by the fitting

$$\chi^2 = \frac{N_{\text{ind}}}{N_{\text{pts}}\varepsilon^2}\sum_{i=1}^{N_{\text{pts}}}\left\{\left[\text{Re}(\tilde{\chi}_{\text{data}}(R_i) - \tilde{\chi}_{\text{th}}(R_i))\right]^2 + \left[\text{Im}(\tilde{\chi}_{\text{data}}(R_i) - \tilde{\chi}_{\text{th}}(R_i))\right]^2\right\}, \quad (2)$$

where N_{pts} is the number of points in the fitted region. The absolute mean-square deviation between the model and experimental spectra was determined by the $\Re$ factor, which was calculated by Eq. (3)

$$\Re = \sum_{i=1}^{N_{\text{pts}}}\frac{\left[\text{Re}(\tilde{\chi}_{\text{data}}(R_i) - \tilde{\chi}_{\text{th}}(R_i))\right]^2 + \left[\text{Im}(\tilde{\chi}_{\text{data}}(R_i) - \tilde{\chi}_{\text{th}}(R_i))\right]^2}{\left[\text{Re}(\chi_{\text{data}}(R_i))\right]^2 + \left[\text{Im}(\chi_{\text{data}}(R_i))\right]^2}. \quad (3)$$

The specific magnetic susceptibility in the solid phase was determined by Faraday's method in a temperature range of 77.4–300 K, and $Hg[Co(CNS)_4]$ was used as a calibration reference [44].

RESULTS AND DISCUSSION

The structure of azomethine H_2L was established by ^1H, ^{13}C, and ^{15}N NMR spectroscopy. According to the elemental analysis data, complexes **Ia**–**Ic** have the composition $(ML)_2$.

The IR spectra of H_2L recorded in KBr pellets, Nujol, and powder (ATR method) contain broad sretching vibration bands at 2870–3426 cm^{-1} due to the ν(OH) and ν(NH) vibrations and absorption bands ν(CH=N) at 1616 cm^{-1}, $\nu_{as}(SO_2)$ at 1341 cm^{-1}, and $\nu_s(SO_2)$ at 1156 cm^{-1}.

Complex formation results in the disappearance of the ν(OH) and ν(NH) sretching vibration bands, a decrease in the ν(CH=N) sretching vibration bands of the ligand by 3–7 cm^{-1}, and the appearance of this band at 1609 (**Ia**), 1612 (**Ib**), and 1610 cm^{-1} (**Ic**). The $\nu_{as}(SO_2)$ and $\nu_s(SO_2)$ sretching vibration bands also decrease to 1296 and 1187 cm^{-1} for **Ib** and to 1301 and 1144 cm^{-1} for **Ic**, respectively.

The formation of the complexes results in the electron density redistribution in the ligand system, which affects the NMR spectra. The following changes are observed when comparing the NMR spectra of compounds H_2L and **Ic**.

The ^1H NMR spectrum of palladium complex **Ic** exhibits no NH^3 (δ = 13.19 ppm) and OH^8 signals (δ = 2.74 ppm) from the ligand protons. The signal from the proton of the azomethine group CH=N undergoes an upfield shift by 1.5 ppm (δ = 7.07 ppm) upon complex formation. The H^{12} signal of the hydroxymethylaniline fragment undergoes the most substantial upfield shift by 1.38 ppm, whereas signals of other protons remain almost unchanged.

Substantial changes upon complex formation are observed in the ^{15}N NMR spectra. The signals of the ligand δ = 306.06 ppm (N^1) and δ = 122.32 ppm (N^3) undergo upfield shifts by 150.3 and 45.6 ppm and appear at δ = 206.3 and δ = 76.7 ppm, respectively.

The ^{13}C NMR spectra exhibit nearly unchanged positions of the signals from the C^{20}, C^{21}, and C^{23} carbon atoms, the downfield shift by 3.97 ppm of the C^{19} signal, and the upfield shift by 3.03 ppm of the C^{22} signal. The C^4 signal from the benzene ring of the aldehyde fragment undergoes the downfield shift by 13.27 ppm, whereas the C^5 and C^6 signals exhibit the upfield shifts by 2.54 and 2.09 ppm, respectively. The highest downfield shift by 10.31 ppm is characteristic of the C^8 signals. The signals of the C^{12}, C^{14}, and C^{17} carbon atoms of the amine fragment of ligand **I** undergo the downfield shifts by 3.84, 1.21, and 6.24 ppm, respectively, upon the formation of palladium complex **Ic**.

Thus, the NMR spectral analysis showed that the signals from the hydrogen, nitrogen, and carbon atoms attached to the $(PdN_2O)_2$ coordination modes underwent the highest changes upon complex formation.

The changes observed in the IR spectra along with the NMR spectral study of ligand H_2L and palladium complex **Ic** indicate the dideprotonation of the ligand upon complex formation and the formation of chelate dimeric structures of complexes **Ia**–**Ic**.

The binuclear character of complexes **Ia** and **Ib** is confirmed by the magnetochemical studies of the copper and cobalt complexes.

The magnetochemical measurements of the complexes in the temperature range from 294 to 77.4 K showed that for **Ia** the magnetic moment was 0.84 μ_B at 294 K and decreased to 0.5 μ_B (77.4 K). For complex **Ib**, μ_{eff} = 4.42 μ_B at 294 K and 3.54 μ_B at 77.4 K. These data indicate the antiferromagnetic exchange interaction between the paramagnetic centers in both complexes.

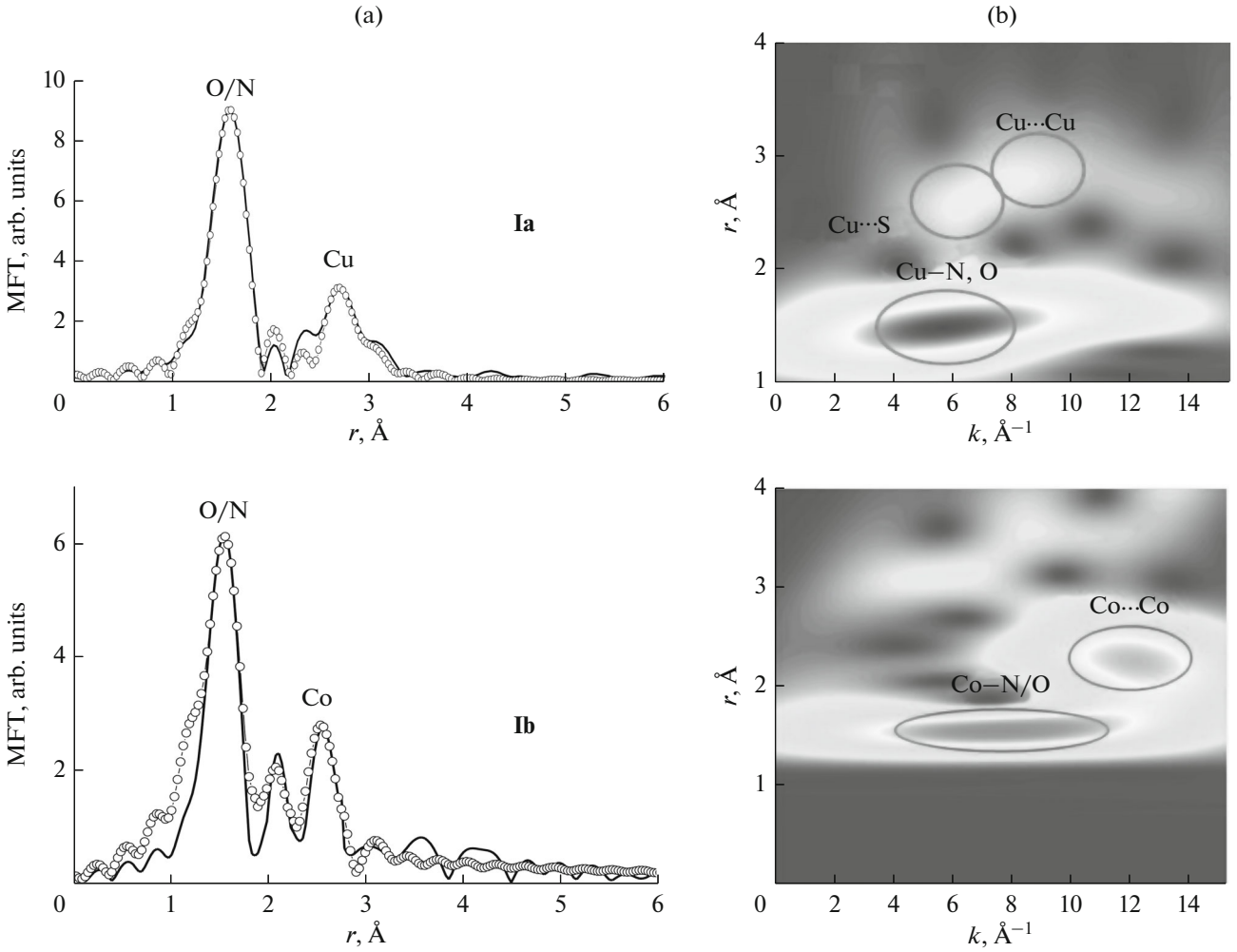

Fig. 1. (a) MFT of the Cu and Co *K*-edge absorption for complexes **Ia** and **Ib** (experiment is shown by solid line, and theory is given by empty circles) and (b) the corresponding WT maps.

In both cases, the temperature dependence of the magnetic susceptibility can be interpreted in the framework of the isotropic model in the isolated dimer approximation, although this dependence is rarely observed for the cobalt(II) complexes because of a significant spin-orbital coupling [45]. For complex **Ia**, the exchange parameter $2J$ calculated by the Bleaney–Bowers equation [46] is -630 cm^{-1} ($g = 2.09$, molar fraction of the paramagnetic impurity $f = 0.084$). For complex **Ib**, the best agreement between the theory and experiment is attained at $J = -21$ cm^{-1} ($g = 2.45$, $f = 0$).

It should be mentioned that complex **Ia** is characterized by a significantly stronger antiferromagnetic exchange interaction between the copper(II) ions compared to its analog containing the hydroxyl group in the phenylamine moiety of the ligand (where $2J = -302$ cm^{-1} [16, 47]) instead of the hydroxymethyl group [16, 35]. A probable reason for this phenomenon is a change in the number of units in the metallocycles: the bridging oxygen atom in complex **Ia** is included into the six-membered metallocycle rather than into the five-membered metallocycle as it takes place in the analog of complex **Ia**.

The binuclear structure of some metal complexes of tridentate azomethine compounds, 2-N-tosylaminobenzaldehyde and salicylaldehyde derivatives with *ortho*-aminophenol and *ortho*-aminothiophenol, was determined earlier by X-ray diffraction analysis [17–22, 24, 27, 31, 38, 48]. These complexes contain binuclear structures with two six-membered and two five-membered metal complexes joined by the oxygen and sulfur bridges. However, in the most cases, crystals of the binuclear complexes suitable for X-ray diffraction cannot be grown. Since attempts to grow crystals of the copper, nickel, and cobalt complexes suitable for X-ray diffraction failed during recent ten years, X-ray absorption spectroscopy is successfully used to establish the dimeric structure of the complexes [22, 24, 26, 28, 29, 34, 35, 48].

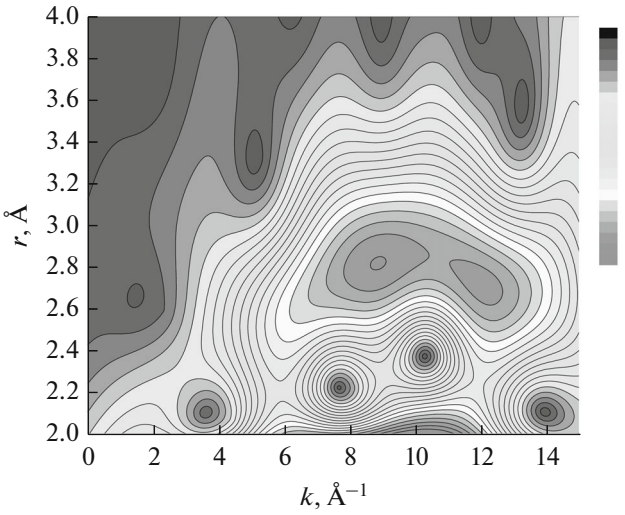

Fig. 2. WT map of the EXAFS wavelet transform for complex **Ia** in the region $r = 2–4$ Å.

The binuclear structures of complexes **Ia** and **Ib** (M = Cu, Co) were confirmed by the fine structure analyses (EXAFS and XANES) of the Cu and Co *K* edges of the X-ray absorption spectra. The wavelet transform (WT) method was also used to analyze the EXAFS function in addition to the traditional approach of spectral analysis using the Fourier transform [49–51]. The WT map of the wavelet transform of EXAFS makes it possible to see the scattering pattern on atoms in both the spatial *r* coordinates and the coordinates of wave vectors *k*, which allows one to separate contributions to scattering from atoms of different types located at the same distance from the absorbing center. The MFT for complexes **Ia** and **Ib** and the corresponding WT maps are shown in Fig. 1.

The MFT of the Cu *K*-edge EXAFS has the main peak at $r = 1.58$ Å, which is due to scattering on the first coordination sphere consisting of the oxygen and nitrogen atoms of the ligand. Another main feature of this MFT is the peak at $r = 2.67$ Å, which can be a candidate for the manifestation of the Cu···Cu distance in this compound. The MFT of the Co *K*-edge EXAFS have peaks at $r = 1.55$ Å (major) and 2.60 Å. The light atoms C, O, and N most efficiently scatter photoelectrons with low wave vectors *k* (scattering maximum at $k = 4–6$ Å^{-1}), whereas the scattering maximum shifts to higher *k* for heavier atoms. The WT maps of EXAFS for compounds **Ia** and **Ib** show that the scattering region of the photoelectron wave has a maximum shifted to higher wave vectors $k = 9–12$ Å^{-1}. Thus, it can be asserted that the second MFT peak corresponds to the distance to the adjacent metal atoms, copper or cobalt, respectively. The WT map for complex **Ia** contains the region corresponding to scattering on the coordinated sulfur atoms of the tosylamine fragment. This is especially well seen for the restricted region of the WT transform $r = 2–4$ Å (Fig. 2).

The quantitative characteristics of the coordination spheres were determined from the multisphere EXAFS approximation. Complex **Ia** was found to have the first coordination sphere consisting of four nitrogen and oxygen atoms at a distance of 1.95 Å and the coordination sphere corresponding to the Cu···Cu distance with $R = 3.03$ Å. The best model of the local structure for complex **Ib** consists of the first coordination sphere of four nitrogen and oxygen atoms with an average Co···N/O distance of 2.05 Å and the coordination sphere corresponding to the Co···Co distance with $R = 2.99$ Å.

Thus, new binuclear Co(II), Cu(II), and Pd(II) complexes were synthesized and their structures were determined by elemental analysis, IR spectroscopy, NMR spectroscopy, and X-ray absorption spectroscopy. The temperature magnetochemical studies of the copper and cobalt complexes indicate their dimeric structures and the strong antiferromagnetic exchange interaction between the metal centers. The dimeric structures of the complexes were also confirmed by the data obtained from an analysis of the X-ray absorption edges of EXAFS. The presence of the hydroxymethyl group instead of the hydroxyl group in the amine moiety of the ligand in the obtained binuclear complexes results in the formation of structures with two six-membered metallocycles (unlike five- and six-membered metallocycles) with the bridging oxygen atoms and leads to the enhancement of the strength of the exchange interaction between the paramagnetic centers.

ACKNOWLEDGMENTS

The IR and NMR experimental data were obtained using the equipment of the Molekulyarnaya spektroskopiya TsKP at the Southern Federal University (Rostov-on-Don, Russia). This work was carried out in the framework of the design part of the state program in the sphere of scientific activities (project no. 4.742.2014/K). The equipment of the Unique Research System "Kurchatov Synchrotron Radiation Source" financed by the Ministry of Education and Science of the Russian Federation (project identifier RFMEFI61914X0002) was used.

REFERENCES

1. Ovcharenko, V.I. and Sagdeev, R.Z., *Russ. Chem. Rev.*, 1999, vol. 68, no. 5, p. 345.
2. Kalinnikov, V.T., Rakitin, Yu.V., and Novotortsev, V.M., *Russ. Chem. Rev.*, 2003, vol. 72, no. 12, p. 995.
3. *Magnetic Molecular Magnetism*, Gatteshi D., Kahn O., Miller J.S., and Palacio F., Eds., Dordrecht: Kluwer Acad., 1985.

4. Pestov, A.V., Slepukhin, P.A., and Charushin, V.N., *Russ. Chem. Rev.*, 2015, vol. 84, no. 3, p. 310.
5. *Magnetism: Molecules to Materials*, Miller J.S. and Drillon, V., Eds., Berlin: Verlag-Chem., 2002.
6. Chaudhury, P., *Coord. Chem. Rev.*, 2003, vol. 243, no. 1, p. 143.
7. Kahn, O., Galy, J., Journaux, Y., and Mongenstern-Badarau, I., *Russ. J. Struct. Chem.*, 1982, vol. 104, no. 18, p. 2165.
8. Levchenkov, S.I., Shcherbakov, I.N., Popov, L.D., et al., *Russ. J. Struct. Chem.,* 2015, vol. 56, no. 1, p. 113.
9. Darensbourg, D.J., Mackiewicz, R.M., Phelps, A.L., and Billodeaux, D.R., *Acc. Chem. Res.*, 2004, vol. 37, p. 836.
10. Ivanchev, S.S., *Russ. Chem. Rev.*, 2007, vol. 76, no. 7, p. 617.
11. Metelitsa, A.V., Burlov, A.S., Bezuglyi, S.O., et al., *Russ. J. Coord. Chem.*, 2006, vol. 32, no. 12, p. 858.
12. Qiao, J., Wang, L.D., and Duan, L., *Inorg. Chem.*, 2004, vol. 43, no. 16, p. 5096.
13. Kogan, V.A., Zelentsov, V.V., Osipov, O.A., and Burlov, A.S., *Russ. Chem. Rev.*, 1979, vol. 48, no. 7, p. 645.
14. Kogan, V.A., Lukov, V.V., and Shcherbakov, I.N., *Russ. J. Coord. Chem.*, 2010, vol. 36, no. 6, p. 401.
15. Burlov, A.S., Antsyshkina, A.S., Romero, Kh., et al., *Zh. Neorg. Khim.*, 1995, vol. 40, no. 9, p. 1480.
16. Garnovskii, A.D., Burlov, A.S., Lukov, V.V., et al., *Russ. J. Coord. Chem.*, 1996, vol. 22, no. 11, p. 786.
17. Garnovskii, A.D., Burlov, A.S., Garnovskii, D.A., et al., *Polyhedron*, 1999, vol. 18, no. 6, p. 863.
18. Antsyshkina, A.S., Sadikov, G.G., Burlov, A.S., et al., *Russ. J. Coord. Chem.*, 2000, vol. 26, no. 10, p. 730.
19. Antsyshkina, A.S., Sadikov, G.G., Burlov, A.S., et al., *Russ. J. Inorg. Chem.*, 2000, vol. 45, no. 11, p. 1666.
20. Garnovskii, D.A., Sadikov, G.G., Antsyshkina, A.S., et al., *Cryst. Rep.*, 2003, vol. 48, no. 3, p. 426.
21. Antsyshkina, A.S., Sadikov, G.G., Burlov, A.S., et al., *Russ. J. Inorg. Chem.*, 2005, vol. 50, no. 3, p. 346.
22. Uraev, A.I., Vasilchenko, I.S., Ikorskii, V.N., et al., *Mend. Commun.*, 2005, vol. 15, no. 4, p. 133.
23. Burlov, A.S., Vlasenko, V.G., Garnovskii, D.A., et al., *J. Struct. Chem.*, 2015, vol. 56, no. 3, p. 504.
24. Burlov, A.S., Koshchienko, Yu.V., Ikorskii, V.N., et al., *Russ. J. Inorg. Chem.*, 2006, vol. 51, no. 7, p. 1065.
25. Burlov, A.S., Ikorskii, V.N., Uraev, A.I., et al., *Russ. J. Gen. Chem.*, 2006, vol. 76, no. 8, p. 1282.
26. Garnovskii, A.D., Ikorskii, V.N., Uraev, A.I., et al., *J. Coord. Chem.*, 2007, vol. 60, no. 14, p. 1493.
27. Burlov, A.S., Koshchienko, Yu.V., Lyssenko, K.A., et al., *J. Coord. Chem.*, 2008, vol. 61, no. 1, p. 85.
28. Burlov, A.S., Ikorskii, V.N., Nikolaevskii, S.A., et al., *Russ. J. Inorg. Chem.*, 2008, vol. 53, no. 10, p. 1566.
29. Burlov, A.S., Nikolaevskii, S.A., Bogomyakov, A.S., et al., *Russ. J. Coord. Chem.*, 2009, vol. 35, no. 7, p. 486.
30. Nikolaevskii, S.A., Burlov, A.S., Bogomyakov, A.S., et al., *Russ. J. Gen. Chem.*, 2012, vol. 82, no. 11, p. 1770.
31. Shmakova, T.O., Garnovskii, D.A., Lysenko, K.A., et al., *Russ. J. Coord. Chem.*, 2009, vol. 35, no. 9, p. 657.
32. Shmakova, T.O., Garnovskii, D.A., Lysenko, K.A., et al., *Izv. Akad. Nauk, Ser. Khim.*, 2009, no. 7, p. 1344.
33. Borisova, A.O., Garnovskii, D.A., Korshunova, E.V., et al., *Izv. Akad. Nauk, Ser. Khim.*, 2012, no. 11, p. 2053.
34. Burlov, A.S., Uraev, A.I., Ikorskii, V.N., et al., *Russ. J. Gen. Chem.*, 2008, vol. 78, no. 6, p. 1230.
35. Burlov, A.S., Uraev, A.I., Garnovskii, D.A., et al., *J. Mol. Struct.*, 2014, vol. 1064, p. 111.
36. Popov, L.D., Tupolova, Yu.P., Lukov, V.V., et al., *Inorg. Chim. Acta*, 2009, vol. 362, no. 6, p. 1673.
37. Garnovskii, A.D., Vasil'chenko, I.S., Garnovskii, D.A., et al., *Ross. Khim. Zh.*, 2009, vol. 53, no. 1, p. 100.
38. Garnovskii, A.D., Burlov, A.S., Vasil'chenko, I.S., et al., *Russ. J. Coord. Chem.*, 2010, vol. 36, no. 2, p. 81.
39. Chernova, N.I., Ryabokobylko, Yu.S., Brudz', V.G., and Bolotin, B.M., *Zh. Org. Khim.*, 1971, vol. 7, no. 8, p. 1680.
40. Chernyshov, A.A., Veligzhanin, A.A., and Zubavichus, Y.V., *Nucl. Instr. Meth. Phys. Res. A*, 2009, vol. 603, p. 95.
41. Kochubei, D.I., Babanov, Yu.A., Zamaraev, L.I., et al., *Rentgenospektral'nyi metod izucheniya struktury amorfnykh tel: EXAFS-spektroskopiya* (*X-Ray Spectral Method for Solid Structure Investigation EXAFS Spectroscopy*), Novosibirsk: Nauka SO, 1988.
42. Newville, M., *J. Synchrotron Rad.*, 2001, no. 8, p. 96.
43. Zabinski, S.I., Rehr, J.J., Ankudinov, A., and Alber, R.C., *Phys. Rev. B: Condens. Matter Mater. Phys.*, 1995, vol. 52, p. 2995.
44. Rakitin, Yu.V. and Kalinnikov, V.T., *Sovremennaya magnetokhimiya* (Modern Magnetochemistry), St. Petersburg: Nauka, 1994.
45. Kahn, O., *Molecular Magnetism*, New York: VCH Publishers, 1993.
46. Bleaney, B. and Bowers, K.D., *Proc. R. Soc. London. A*, 1952, vol. 214. no. 1119, p. 451.
47. Uraev, A.I., *Doctoral (Chem.) Dissertation*, Rostov-on-Don: Southern Federal Univ., 2014.
48. Garnovskii, D.A., Antsyshkina, A.S., Churakov, A.V., et al., *Russ. J. Inorg. Chem.*, 2014, vol. 59, no. 5, p. 431.
49. Funke, H. and Chukalina, M., *FZR Annual Reports*, 2001, vol. 343, p. 45.
50. Funke, H., Scheinhost, A.C., and Chukalina, M., *Phys. Rev. B*, 2005, vol. 71, p. 094110.
51. Funke, H., Chukalina, M., and Scheinost, A.C., *J. Synchrotron Rad*. 2007, vol. 14, p. 426.

Translated by E. Yablonskaya